



**THE ELECTROMAGNETIC AND HADRONIC
DIFFRACTIVE DISSOCIATION OF ^{16}O IONS**

G. Baroni^h, V. Bisi^j, A.C. Breslin^c, D.H. Davis^f, S. Di Liberto^h, G. Grellaⁱ,
K. Hoshino^g, M. Kazuno^d, K. Kodama^g, A. Marzari-Chiesa^j, M.A. Mazzoni^b, F. Meddi^h,
M.T. Muciaccia^a, K. Niu^g, L. Ramello^j, G. Romanoⁱ, G. Rosa^h, M.S. Sartori^j,
C. Sgarbi^h, H. Shibuya^d, S. Simone^a, D.N. Tovee^f, N. Ushida^e, T. Virgili^h, C. Wilkin^f
and S.K.C. Yuen^f.

Abstract

Events which satisfy the kinematics of $p(^{16}\text{O}, \text{CHe}p)$, with low excitation energy in the (CHe) system and a low-energy recoil proton, have been identified in the interactions of 200 GeV per nucleon ^{16}O ions with nuclear emulsion. An eikonal distorted-wave impulse approximation (DWIA) estimate of the target A dependence of strong interaction diffractive dissociation suggests that, on the basis of these hydrogen data, most of the (CHe) final states, previously ascribed to electromagnetic dissociation on heavy nuclei, might rather be hadronic in character. This contamination is very much less important in the dominant (NH) channel.

Submitted to Nuclear Physics A

-
- a)* Dipartimento di Fisica dell'Università and INFN, Bari, Italy.
 - b)* CERN, Geneva, Switzerland.
 - c)* Department of Physics, University College, Dublin, Ireland.
 - d)* Department of Physics, Toho University, Funabashi, Japan.
 - e)* Aichi University of Education, Kariya, Japan.
 - f)* Department of Physics and Astronomy, University College London, London, UK.
 - g)* Department of Physics, Nagoya University, Nagoya, Japan.
 - h)* Dipartimento di Fisica, Università 'La Sapienza' and INFN, Rome, Italy.
 - i)* Dipartimento di Fisica Teorica e SMSA dell'Università and INFN, Salerno, Italy.
 - j)* Dipartimento di Fisica dell'Università and INFN, Turin, Italy.

1 INTRODUCTION

A previous work [1] showed that events for which all that was observed was the low-energy breakup of the projectile accounted for a significant fraction of the interactions of ultra-relativistic heavy ions in their passage through nuclear emulsions. At 200 GeV per nucleon these were 11% of the total in the case of ^{16}O and 18% for ^{32}S . These events were ascribed to electromagnetic dissociation (EMD) processes in the Coulomb field of the target nuclei within the emulsion.

Charge and angular measurements allowed these events to be categorized into various breakup channels and the excitation energies of the final nucleus to be estimated. By assuming a virtual photon spectrum given by the prescription of Weiszäcker and Williams [2]–[4] and corresponding to the nuclear elements in the emulsion, it was then possible to compare the cross-sections for various channels with the results obtained from real photon events, where available. Whereas there was good agreement for both the ^{16}O and ^{32}S results for (γ, p) processes, especially in the giant dipole region, the EMD cross-sections for (γ, α) processes were an order of magnitude larger than expected. It was mooted [1] that a possible explanation for this discrepancy could be in terms of a contribution from multiphoton processes. It should though be borne in mind that conventional estimates of these suggest that, in general, they should be small [5].

However, events have been observed, which seem to have all the features ascribed to electromagnetic breakup, except that at the point of dissociation there is also a track of a very-low-energy charged particle. Indeed, on measurement, some of the events were found to be consistent with diffractive dissociation on free protons within the emulsion. It is highly unlikely, because of the proton's small charge, that these could in fact be electromagnetic in origin and so they must be induced by the strong interaction. In view of this, a careful search was performed on a much extended sample of 200 GeV per nucleon ^{16}O ion interactions to establish the extent of such processes, particularly those giving rise to (C He) and (N H) final states of the ^{16}O nucleus. Since we have no isotope identification in the emulsion it is impossible to separate ^1H from ^2H or ^3He from ^4He . However, it is expected that most of the H and He in the final states will be protons and ^4He (α) respectively. The procedures and results of this search are presented in section 2, where it is shown that about 12% of the (C He) final states are consistent with being produced on hydrogen whereas for (N H) the figure is less than 1%.

Similar coherent hadronic processes occurring on nuclei other than hydrogen in the emulsion would produce no recognizable recoil and so such events would thus be kinematically indistinguishable from those originally classified as being electromagnetic.

On the other hand, it is very difficult to make an *a priori* theoretical estimate of the hadronic diffractive dissociation cross-section because of the complexity of the nuclear physics of ^{16}O at high (10–20 MeV) excitation energies. Not only would one need a good description of the transition form factor to the various nuclear levels, but also the results are heavily dependent on their branching ratios into the (C He) final state. There is though sufficient information to make reliable estimates of the excitation of the 2^+ level of ^{16}O at 11.52 MeV for both the hydrogen and complex nuclear targets. The calculations, described in detail in section 3, show that in the hydrogen case about 13% of the observed events would be expected to excite this one particular nuclear level. The resulting predicted target dependence is quite close to the $A^{1/3}$ expected from production by a rim around the nucleus. As a consequence, about 11% of the events previously classified as EMD on emulsion nuclei are likely to arise from strong interaction excitation of this specific level.

Since it is impractical to make reliable estimates for the other levels and the continuum, we must make the simplifying assumption that this particular level is typical of all the levels produced by diffractive dissociation. In particular, we assume that the A dependence is as given in the model calculation for the 2^+ state so that we can estimate the number of strong interaction events to be expected in the emulsion by using this A dependence to scale from our hydrogen results. It is shown in the conclusions of section 4 that such a scaling predicts a number of (CHe) events which is close to that which we have observed experimentally! It appears therefore that there is a very large hadronic contribution to (CHe) final states in the diffractive breakup of relativistic ^{16}O ions on nuclei but that this contamination is far less serious for the dominant (NH) final states.

2 EXPERIMENTAL PROCEDURES AND RESULTS

The experimental set-up and the line-scanning procedures used to locate interactions of ^{16}O ions in emulsion and the measurements made are fully described in an earlier paper of ours [6]. The particular selection made to establish the electromagnetic sample of events is given in ref. [1]. However, additional scanning has been made, in some plates for all classes of interactions and in others for only those satisfying the EMD classification [1]. As a consequence, the various classes of events discussed in this paper are obtained from the different track length samples given in table 1. Thus a further 508 m of 200 A GeV ^{16}O track have been added to those obtained from the original 349 m used earlier [1], resulting in 85 and 503 events classified as EMD candidates for (CHe) and (NH) final states, respectively, with estimated excitation energies of less than 150 MeV. These estimates of the total centre-of-mass kinetic energy E released in the interactions were made assuming isotropy as in ref. [1].

Interactions leading to hadronic dissociation of ^{16}O on hydrogen are to be found among the sample scanned for nuclear interactions. They have a topology characteristic of an EMD event plus a track of a low-energy single-charged particle at the interaction vertex. The direction of such a track with respect to the primary beam was measured, as well as its range where possible. The method of development and subsequent sticking of the emulsion pellicles on glass may result in local distortions which can affect the determination of the track angles, particularly those of steeply inclined tracks. If this effect were observed to be present for any event, the coordinates of the points measured on the 'proton' track were corrected following an extension of the method of Apostolakis and Major [7], and the emission angles redetermined. Such distortions do not affect the measurements of the small opening angle between the particles from the breakup of the ^{16}O ion. In some cases the range could not be measured as the proton left the emulsion stack before coming to rest. However, in each case it was judged, from an examination of its ionization and scattering, to be close to rest. Consequently, only a small underestimate of the proton's momentum is incurred by using the observed track length. An estimate of the total centre-of-mass kinetic energy E released in the breakup of the ^{16}O was also made.

Eleven examples of the topology (CHe + a low energy 'proton') were located. The details of these events are listed in table 2. To be kinematically consistent with the diffractive dissociation of an ^{16}O ion on a free proton within the emulsion, the magnitude of the

‘proton’ momentum q and its emission angle θ with respect to the beam direction should satisfy, to a good approximation, the relation

$$\cos(\theta) = \frac{q}{2m}, \quad (1)$$

where m is the mass of the struck proton. The nine events satisfying this condition also have a centre-of-mass kinetic energy spectrum similar to that of the 85 events classified as EMD (CHe) candidates, as shown in fig. 1a. The other two events, which do not satisfy the free hydrogen criterion, may correspond to the knock-out of a proton from a heavier nucleus in the emulsion. The kinematic relation of eq. (1) would then be modified by both the Fermi motion of the proton in the nucleus and its multiple scattering while emerging therefrom.

The situation with regard to the so-called (NH + a low energy ‘proton’) events is far less clear because in this case one cannot distinguish between the tracks of a forward-going fast proton and a produced charged pion on the basis of ionization alone. Nevertheless, nine events with the correct scanning topology were found. The details of these events are given in table 3. Six of them were kinematically consistent with production on free hydrogen. It is, however, only in two cases that the opening angle between the nitrogen and the supposed forward-going proton is such as to give an excitation energy in the ^{16}O system of less than about 50 MeV, the region in which 96% of our EMD (NH) candidates lie, as clearly demonstrated by fig. 1b. The remaining events, therefore, do not look typical of electromagnetic dissociation. It is in fact likely that in most of these cases the minimum-ionizing single-charged particle is actually a pion rather than a stripped projectile proton, since at large outgoing angles a 200 GeV proton would have a larger than expected transverse momentum.

3 THEORETICAL PREDICTIONS

3.1 Formalism

In the distorted-wave impulse approximation (DWIA) for the excitation of nucleus B in the reaction $A + B \rightarrow A + B^*$, the transition from the ground to the excited state is assumed to take place in a single step but with a purely elastic distortion coming before and after the transition. At high energies it is legitimate to evaluate such a distortion in the eikonal approximation [8, 9], the resulting amplitude then corresponding to the dominant subset of terms given by the Glauber theory [10].

If we neglect the spin and isospin dependence of the high-energy nucleon–nucleon amplitudes $f_{\text{NN}}(q)$ then the amplitude for the excitation of a state of angular momentum ℓ and projection m in nucleus B is

$$F_{\ell m}(\vec{q}) = \sqrt{4\pi} f_{\text{NN}}(0) \int e^{i\vec{q}\cdot\vec{r}} D(b) Y_{\ell m}(\hat{r}) \rho_{\ell}^{\text{tr}}(r) d^3r, \quad (2)$$

where it is assumed that both A and B are of spin zero.

In the eikonal approximation the trajectory is a straight line at a constant impact parameter vector \vec{b} , so that in the integration $\vec{r} = (\vec{b}, z)$. The distortion factor

$$D(b) = e^{i\chi(b)} \quad (3)$$

is then given by an integral over the momentum transfer \vec{q} ,

$$\chi(b) = \frac{AB}{2\pi^{3/2}} \int e^{-i\vec{q}\cdot\vec{b}} S_A(q) S_B(q) f_{\text{NN}}(q) d^2q. \quad (4)$$

Here S_A and S_B are the ground-state point matter form factors of the two nuclei with A and B nucleons respectively.

To avoid frame transformations the amplitudes are normalized to the momentum transfer such that

$$\left(\frac{d\sigma}{dq^2}\right)_{\ell m} = |F_{\ell m}(\vec{q})|^2 . \quad (5)$$

In the absence of distortion, $D(b) = 1$, it is convenient to quantize along the direction of the momentum-transfer vector \vec{q} , and in this limit one recovers the plane wave impulse approximation result

$$F_{\ell m}^{\text{PW}}(q) = A B \sqrt{2\ell + 1} i^{-\ell} S_A(q) S_B^{\text{tr}}(q) f_{\text{NN}}(q) \delta_{m,0} , \quad (6)$$

where $S_B^{\text{tr}}(q)$ is the transition matter form factor to the excited state.

The comparison of eqs. (2) and (5) allows us to evaluate the effective nuclear transition density

$$\rho_{\ell}^{\text{tr}}(r) = \frac{\sqrt{4\pi}}{(2\pi)^3} A B \int S_A(q) S_B^{\text{tr}}(q) \frac{f_{\text{NN}}(q)}{f_{\text{NN}}(0)} j_{\ell}(qr) q^2 dq , \quad (7)$$

which therefore depends upon the shape of the nucleon–nucleon amplitude as well as nuclear structure information.

At high energies the nucleon–nucleon amplitude is dominated by the imaginary part and the diffraction peak may be parametrized as

$$f_{\text{NN}}(q) = \frac{i\sigma_{\text{NN}}}{4\sqrt{\pi}} e^{-\beta^2 q^2/2} , \quad (8)$$

where, with the normalization of eq. (5), σ_{NN} is the total nucleon–nucleon cross-section.

3.2 Application to ^{16}O scattering

It has been shown that the elastic ^{16}O form factor is well described by harmonic oscillator wave functions with an r.m.s. charge radius of 2.72 fm [11]. In the inelastic case there are three low-lying 2^+ states of ^{16}O whose transition form factors have been well measured in electron scattering [12]. The 2_1^+ and 2_3^+ levels at 6.92 and 11.52 MeV respectively have form factors which are almost identical in shape, corresponding to surface-peaked transition densities, though the amplitude of the latter is about $1/\sqrt{2}$ smaller. After removing the proton size the form factors can be parametrized as

$$S_{2_1^+}(q) = 0.1844 q^2 (1 - q^2/1.935^2) e^{-0.80 q^2} \quad (9)$$

$$S_{2_3^+}(q) = 0.1217 q^2 (1 - q^2/1.970^2) e^{-0.72 q^2} . \quad (10)$$

On the other hand, the overlap for the 2_2^+ state at 9.85 MeV is peaked in the interior so that its B2 moment is quite small and we shall not consider it further. Since the threshold for α decay is at 7.16 MeV, the 2_1^+ cannot be seen in the (^{12}C α) mode, whereas the 2_3^+ decays essentially 100% in this way and might therefore be seen in our experiment.

The factor of 2 between the 6.92 and 11.52 MeV levels is also seen in proton scattering at 200 and 500 MeV [13, 14], where the shapes of the two cross-sections are found to be very similar.

Experimental data exist on the excitation of only the (lower) 2_1^+ level by proton scattering at 800 MeV [15]. The eikonal DWIA formalism outlined above should be equally

valid for proton scattering providing the nuclear form factor $S_A(q)$ is put equal to unity. The parameters are a little ambiguous in view of the neglect of the spin and isospin dependence as well as the real part of the NN amplitudes at such a low energy. Nevertheless, taking $\sigma_{NN} = 4.0 \text{ fm}^2$ and $\beta^2 = 0.2 \text{ fm}^2$, the very satisfactory agreement shown in fig. 2 is obtained. This reproduces well both the shape and the absolute normalization of the cross-section, and confirms that both the reaction mechanism and nuclear structure information are sufficiently well understood to make reliable estimates for *both* 2^+ levels.

The validity of the eikonal DWIA model should improve with energy, and when applied at our energy of 200 GeV per nucleon using $\sigma_{NN} = 3.9 \text{ fm}^2$ and $\beta^2 = 0.44 \text{ fm}^2$ [16] it predicts an integrated cross-section for the 11.52 MeV level of

$$\sigma[{}^{16}\text{O p} \rightarrow {}^{16}\text{O}^*(11.52) \text{ p}] = 0.52 \text{ mb} , \quad (11)$$

which would be seen finally in the ${}^{12}\text{C} + \alpha$ channel. The shape of the distribution in q^2 is broadly similar to the lower energy results of fig. 2 with an r.m.s. value of $\langle q^2 \rangle^{1/2} = 200 \text{ MeV}/c$. The corresponding figure for the 9 hydrogen events shown in table 1 is $213 \pm 76 \text{ MeV}/c$.

On the basis of this cross-section estimate and the path length scanned, we would expect to have 1.2 events where the final ${}^{16}\text{O}$ nucleus is found in this one excited state. The total cross-section deduced from the nine events listed in table 2 is $4.0 \pm 1.4 \text{ mb}$. Thus this particular 2^+ level accounts for about 13% of the (C He p) events that were discussed in section 2. Such a modest figure is not surprising in view of the myriad of higher energy ${}^{16}\text{O}$ levels which have significant branching ratios to $({}^{12}\text{C} \alpha)$ [17].

Turning now to the interaction of the oxygen ions with the heavier components in the emulsion, the calculations proceed identically except that the elastic form factor for the target nucleus $S_A(q)$ has to be included. Evaluating this with harmonic oscillator densities for the light (C,N,O) nuclei and Wood-Saxon densities for the heavy (Br,Ag), the predicted integrated cross-sections for $\sigma({}^{16}\text{O A} \rightarrow {}^{16}\text{O}^* \text{ A})$, where the target nucleus A is left in its ground state, are shown in fig. 3. Such events should have a rather steeper q dependence than for hydrogen, but any such coherent recoils would be completely unrecognizable in the emulsion. In view of the strong damping and the large nuclear sizes, only the rim of the nucleus should contribute to such excitations so that a behaviour of roughly $A^{1/3}$ would be expected. In fact a log-log fit to the results of our calculations in fig. 3 is quite close to this with

$$\sigma({}^{16}\text{O A} \rightarrow {}^{16}\text{O}^* \text{ A}) = 0.865 A^{0.29} = 1.65 \sigma_p A^{0.29} \text{ mb} . \quad (12)$$

There is, of course, no reason for this form to be valid for hydrogen since the rim there encompasses the majority of the target!

From the proportions of the different nuclear species in our emulsion stack given in ref. [6], it is straightforward to derive from eq. (12) the relative number of events expected on medium/heavy nuclei as compared to those on hydrogen. This turns out to be

$$\frac{N(A > 1)}{N(A = 1)} = 6.1 . \quad (13)$$

There should therefore be about 10 events corresponding to the excitation of this single nuclear level via the *strong* interactions where the elastically recoiling target nucleus would not have been recognized.

From an inspection of the distribution of the c.m. energy E of the (CHe) events given in fig. 1a, it is seen that there are cases where the kinetic energy in the $\alpha-^{12}\text{C}$ system is of the order of 4 MeV so that they could correspond to this level. However, the majority are at higher excitation energies where there is no immediate prospect of evaluating DWIA cross-sections since the corresponding electromagnetic form factors have not been studied in detail for ^{16}O excitation energies above 12.1 MeV [12].

4 CONCLUSIONS

We have shown in the previous section that, within the framework of an eikonal DWIA analysis, a significant fraction of the low excitation (CHe) events produced on either hydrogen or heavier nuclei may be associated with the 11.52 MeV level in ^{16}O . However, lack of nuclear-structure information precludes a similar estimation of the excitation of higher nuclear levels. In view of this impasse, the simplest hypothesis that we can make is that these higher levels behave broadly similarly to the 2^+ ones and in particular that the A dependence is given by eq. (12). In that case we can take the number of events that we have observed on free hydrogen (assuming that owing to the small charge these are *not* of electromagnetic origin) and scale to the other target nuclei using the 6.1 factor of eq. (13). This scaling might still be reasonable if some of the events that we observe correspond, for example, to the production of ^3He rather than ^4He .

The predicted number of hadronic events where there is no observable low-energy recoil should be

$$N(\text{CHe}) = (9 \pm 3) \times 6.1/0.74 = 74 \pm 25 , \quad (14)$$

where the 0.74 denominator arises from the fraction of the track length scanned for these events. The quoted error is only statistical, arising purely from the number of hydrogen events. This scaling suggests that the bulk of the 85 EMD candidates in this channel described in section 2 should in fact be of strong interaction origin. In addition though, there are likely to be cases where the nucleus A is excited through the strong interactions and the final two knock-out events of table 1 look like examples of this category. After these subtractions have been made our results would not be in disagreement with an estimate based on data from real photons which predicts about 9 events [1]. In principle, there should be interference terms between the electromagnetic and hadronic excitations, but these are probably very small owing to the latter being dominantly imaginary with the former being dominantly real.

In the case of the (NH) events we have found only two events on hydrogen which could satisfy the EMD criteria, corresponding to a cross-section of 1.2 ± 0.8 mb. On this basis we would only expect of the order of $2 \times 6.1/0.54 = 23 \pm 16$ events on the complex nuclei in the emulsion. This is small compared to the 503 events reported in section 2 and so changes little the plausible agreement with real (γ, p) data shown in ref. [1]. Hence there seems to be little in these two-body breakup channels which is not to be expected on the basis of low-energy nuclear physics information.

It is very hard to devise useful criteria for the selection of EMD events, but at high energies the strong interactions will only populate the isospin $T=0$ states of ^{16}O . This is to be contrasted with the case of electromagnetic excitation which can lead to those with both $T=0$ and $T=1$. Coupled with the relatively small cross-section for the reaction $p(^{16}\text{O}, \text{NH}p)$ compared to $p(^{16}\text{O}, \text{CHe}p)$ this suggests that the states of ^{16}O which decay into $^{15}\text{N}p$ must be mainly of isospin 1 or otherwise we would have found more (NH p) events. However, one must bear in mind that experimentally we have no

isotope identification or efficient neutron detection and theoretically there are a multitude of low-lying energy levels in ^{16}O . This precludes detailed nuclear physics calculations of the relative proportion of these excited states decaying via the (CHe) and (NH) channels.

Experimentally, we have not considered a detailed examination of events of the type $^{32}\text{S} p \rightarrow ^{28}\text{Si} \text{He} p$ worth while as we have not been able to augment our sample of 27 (SiHe) EMD candidates of ref. [1]. In addition, the low excitation (SiHe) states of ^{32}S cannot be studied theoretically in the same manner as for the ^{16}O ones because of the poor knowledge of the electromagnetic transition form factors for the ^{32}S nucleus. However, despite this inability to predict the absolute cross-section for this process, its dependence on target mass is expected to be similar to that of ^{16}O projectiles which, when expressed as a function of target charge Z is of the form $Z^{0.31}$. This is markedly different from the Z^2 behaviour expected for pure EMD processes. This difference, which arises from the much longer range at high energies of electromagnetic as compared to hadronic excitation, can be explored in our current experiment EMU09 [18], which detects EMD reactions from a variety of foil targets of widely different atomic numbers.

Acknowledgements

We are grateful to our scanning teams for their patience and efficiency. Conversations with L. Castillejo and correspondence with G. Baur have been very helpful.

Support from the Mitsubishi Foundation, from the Japan Society for the Promotion of Science, and from the Monbusho International Scientific Research Program is greatly appreciated.

REFERENCES

- [1] G. Baroni et al., Nucl. Phys. **A516** (1990) 673.
- [2] C.F. von Weiszäcker, Z. Phys. **88** (1934) 612.
- [3] E.J. Williams, Phys. Rev. **45** (1934) 729.
- [4] J.D. Jackson, Classical electrodynamics, 2nd edn. (Wiley, NY, 1975).
- [5] C.A. Bertulani and G. Baur, Phys. Lett. **B174** (1986) 23.
- [6] G. Baroni et al., Nucl. Phys. **A531** (1991) 691.
- [7] A.J. Apostolakis and J.V. Major, Brit. J. Appl. Phys **8** (1957) 9.
- [8] H.K. Lee and H. McManus, Phys. Rev. Lett. **20** (1968) 337.
- [9] C. Rogers and C. Wilkin, Nuovo Cimento Lett. **1** (1971) 575.
- [10] R.J. Glauber, *in* Lectures in Theoretical Physics, Vol. 1, Ed. W.E. Brittin (Interscience Publishers, NY, 1959), p.315.
- [11] C. Hyde-Wright et al., Phys. Rev. **C35** (1987) 880.
- [12] T.N. Buti et al., Phys. Rev. **C33** (1986) 755.
- [13] J.J. Kelly et al., Phys. Rev. **C41** (1990) 2504.
- [14] B.S. Flanders et al., Phys. Rev. **C43** (1991) 2103.
- [15] G.S. Adams et al., Phys. Rev. Lett. **43** (1979) 42.
- [16] M.K. Carter, P.D.B. Collins and M.R. Whalley, Rutherford Appleton Laboratory compilation RAL-86-002 (1986).
- [17] F. Ajzenberg-Selove, Nucl. Phys. **A460** (1986) 1.
- [18] N. Armenise et al. (EMU09 Collaboration), Proposal CERN/SPSC/89-1, P-243 (1989).

Table 1

Number of events and associated track lengths for various classes of events

Class	Total track length examined (m)	Number of events
^{16}O (nucleus) \rightarrow C He (nucleus)	857.2	85
^{16}O (nucleus) \rightarrow NH (nucleus)	857.2	503
^{16}O p \rightarrow C He p	635.3	11 ^{a)}
^{16}O p \rightarrow NH p	463.0	9 ^{b)}

^{a)} See details in table 2.^{b)} See details in table 3.

Table 2

Events satisfying the C He p topology. The nine above the horizontal line satisfy the kinematics of $^{16}\text{O} p \rightarrow ^{12}\text{C} \alpha p$

Proton range (μm)	Proton momentum (MeV/c)	Observed emission angle ($^\circ$)	Predicted emission angle ($^\circ$)	Energy E above $^{12}\text{C} \alpha$ threshold (MeV)
294	112	83.3 ± 2.8	86.6	8.7
1636	185	84.3 ± 2.2	84.3	18.6
> 7322 ^{a)}	$\gtrsim 286$	81.1 ± 0.9	$\lesssim 81.3$	11.8
173	95	81.2 ± 3.3	87.1	8.4
> 10200 ^{a)}	$\gtrsim 315$	74.4 ± 2.2	$\lesssim 80.3$	17.6
2401	207	85.1 ± 1.5	83.7	2.2
> 1154 ^{a)}	$\gtrsim 167$	82.4 ± 1.4	$\lesssim 84.9$	28.0
> 4500 ^{a)}	$\gtrsim 248$	85.6 ± 2.6	$\lesssim 82.4$	6.5
2125	200	82.9 ± 2.1	83.9	7.2
381	121	147.0 ± 2.2	86.3	16.3
208	101	107.4 ± 3.1	86.9	1.9

^{a)} In these events the proton leaves the emulsion but it is already close to rest. The estimated residual range is less than 1 mm, which would imply only a small increase in the initial proton momentum.

Table 3

Events satisfying the NH p topology. Only the two above the horizontal line satisfy the kinematics of $^{16}\text{O} p \rightarrow ^{15}\text{N} p p$ with a value of the excitation energy compatible with electromagnetic dissociation

Proton range (μm)	Proton momentum (MeV/c)	Observed emission angle ($^\circ$)	Predicted emission angle ($^\circ$)	Energy E above $^{15}\text{N}p$ threshold (MeV)
425	125	92.6 ± 3.0	86.2	6.8
3170	224	84.0 ± 1.5	83.1	20.1
$> 4693^{\text{a)}$	$\gtrsim 251$	79.9 ± 0.8	$\lesssim 82.3$	51.0
$> 9345^{\text{a)}$	$\gtrsim 307$	79.6 ± 1.2	$\lesssim 80.6$	90.9
$> 1820^{\text{a)}$	$\gtrsim 191$	70.1 ± 2.3	$\lesssim 84.2$	106.9
12005	330	79.9 ± 1.0	79.9	122.7
442	126	91.3 ± 3.7	86.2	273.9
$> 12650^{\text{b)}$	$\gtrsim 335$	87.4 ± 0.8	$\lesssim 79.7$	493.1
126	86	147.0 ± 4.5	87.4	908.8

Note: In these events the proton leaves the emulsion but it is already close to rest. The estimated residual range is less than 1 mm^{a)} or 2 mm^{b)}, respectively, which would imply only a small increase in the initial proton momentum.

Figure Captions

Fig. 1: Centre-of-mass energy spectra of candidates for EMD (open histogram) and hadronic diffraction on free protons (shaded histogram) of (a) (CHe) and (b) (NH) final states. For clarity, the ordinate for the (NH p) events has been scaled by a factor of 20.

Fig. 2: Experimental cross-sections for $p \text{ }^{16}\text{O} \rightarrow p' \text{ }^{16}\text{O}^*(6.92)$ at 800 MeV [15] are compared with the predictions of the eikonal DWIA calculation described in section 3.

Fig. 3: Predicted integrated cross-section for $^{16}\text{O} \text{ A} \rightarrow ^{16}\text{O}^*(11.52) \text{ A}$ on various emulsion nuclei at 200 GeV per nucleon. The parameters of the straight line log-log fit are given in eq. (12).

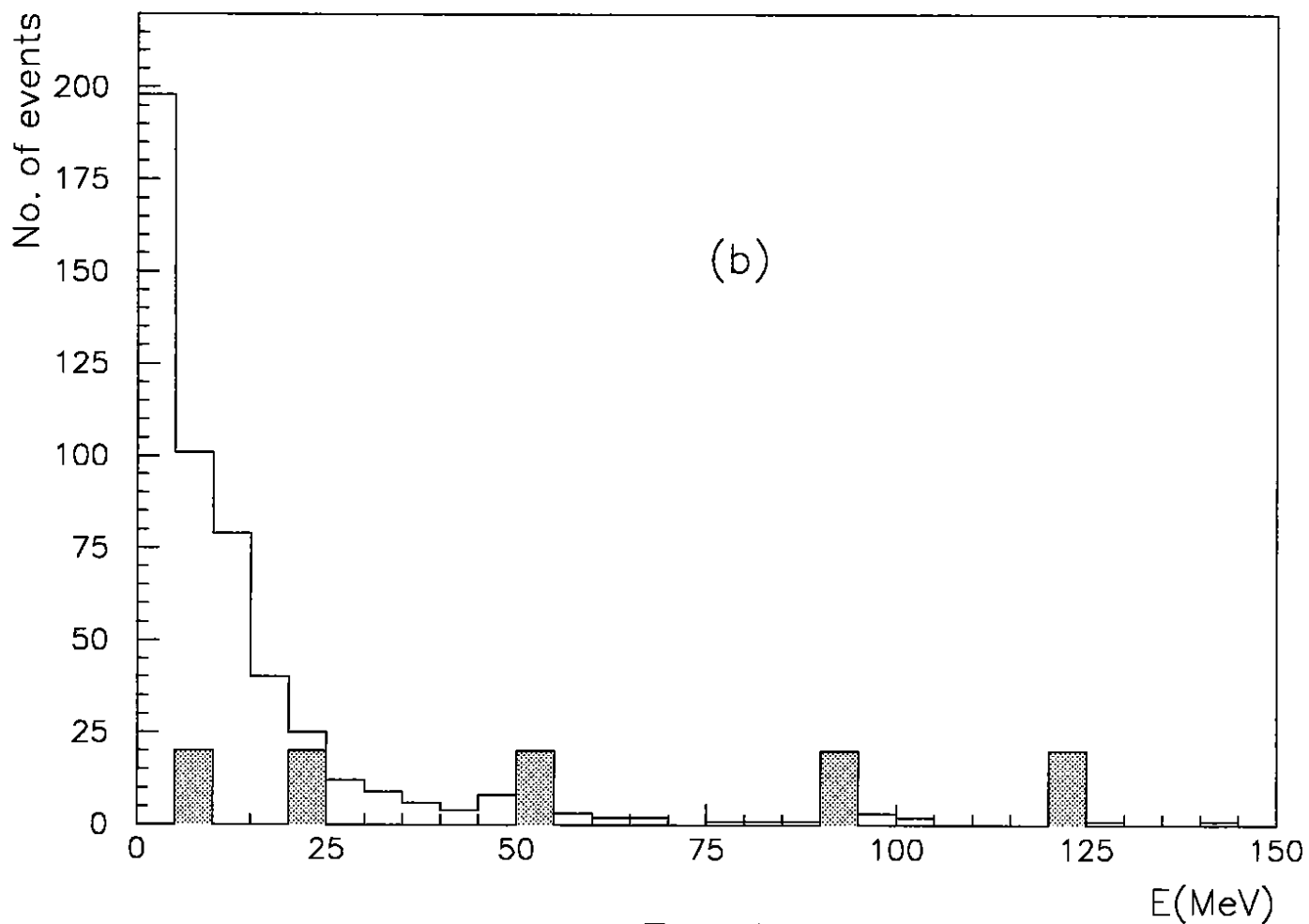
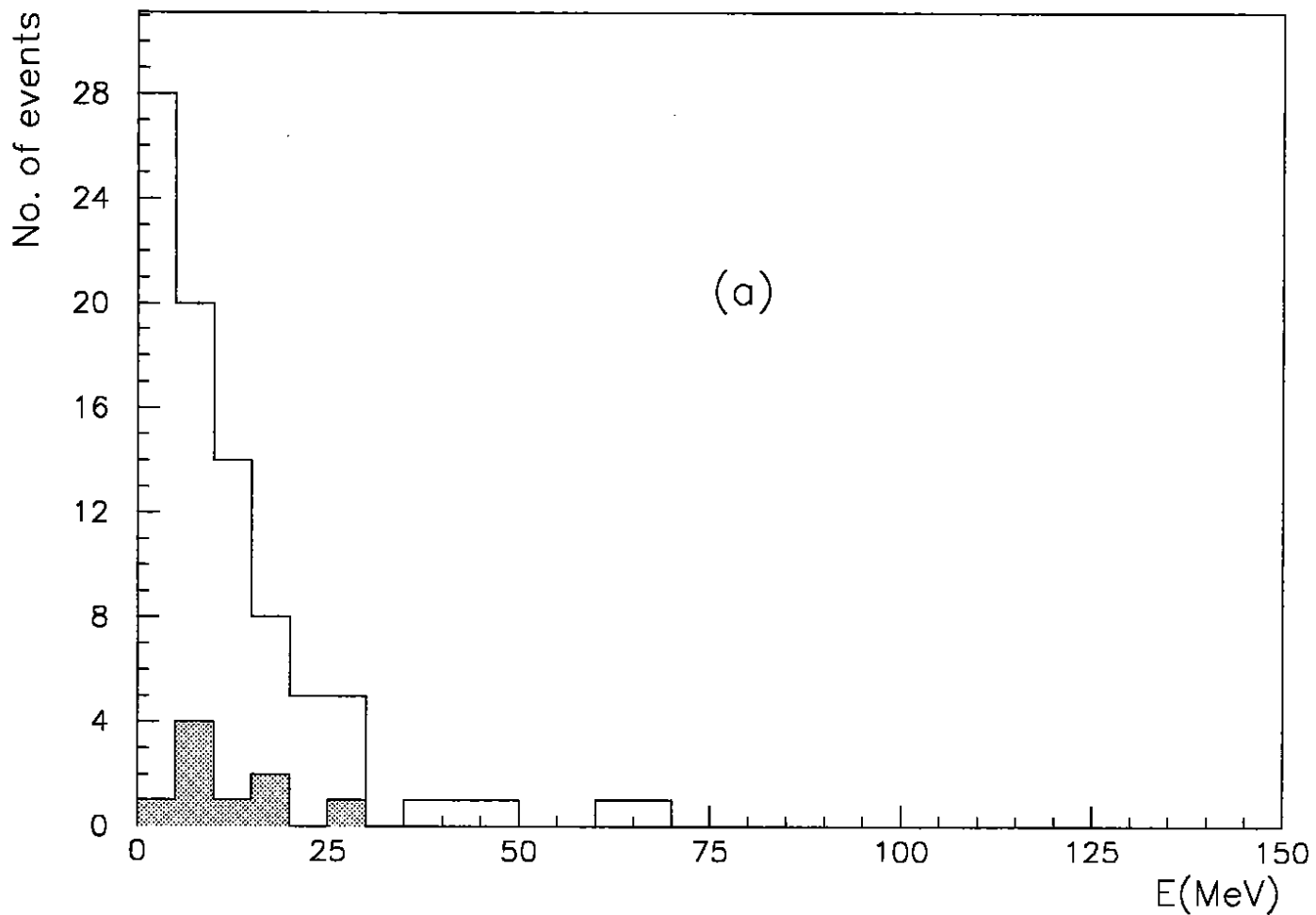


FIG. 1

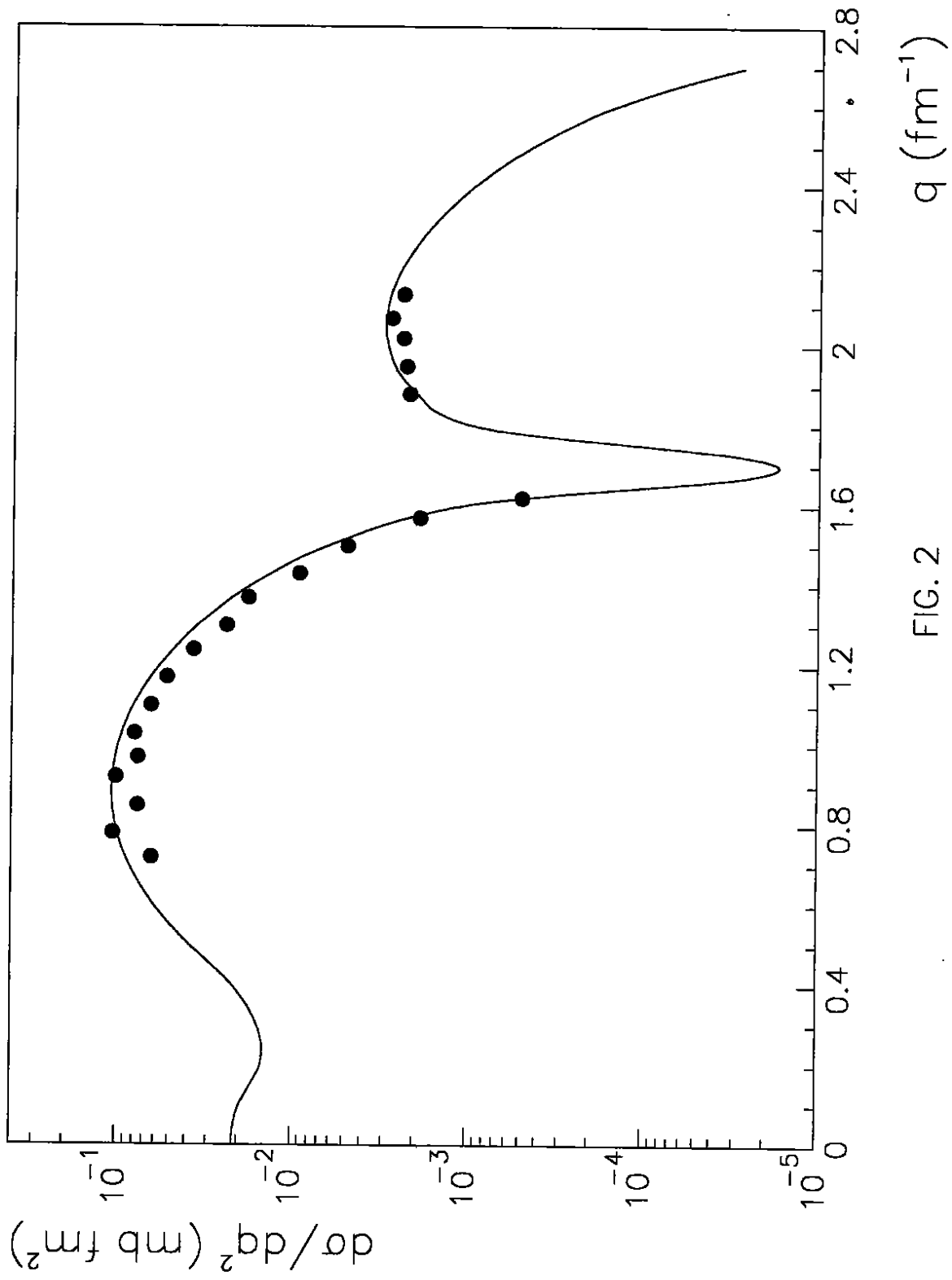


FIG. 2

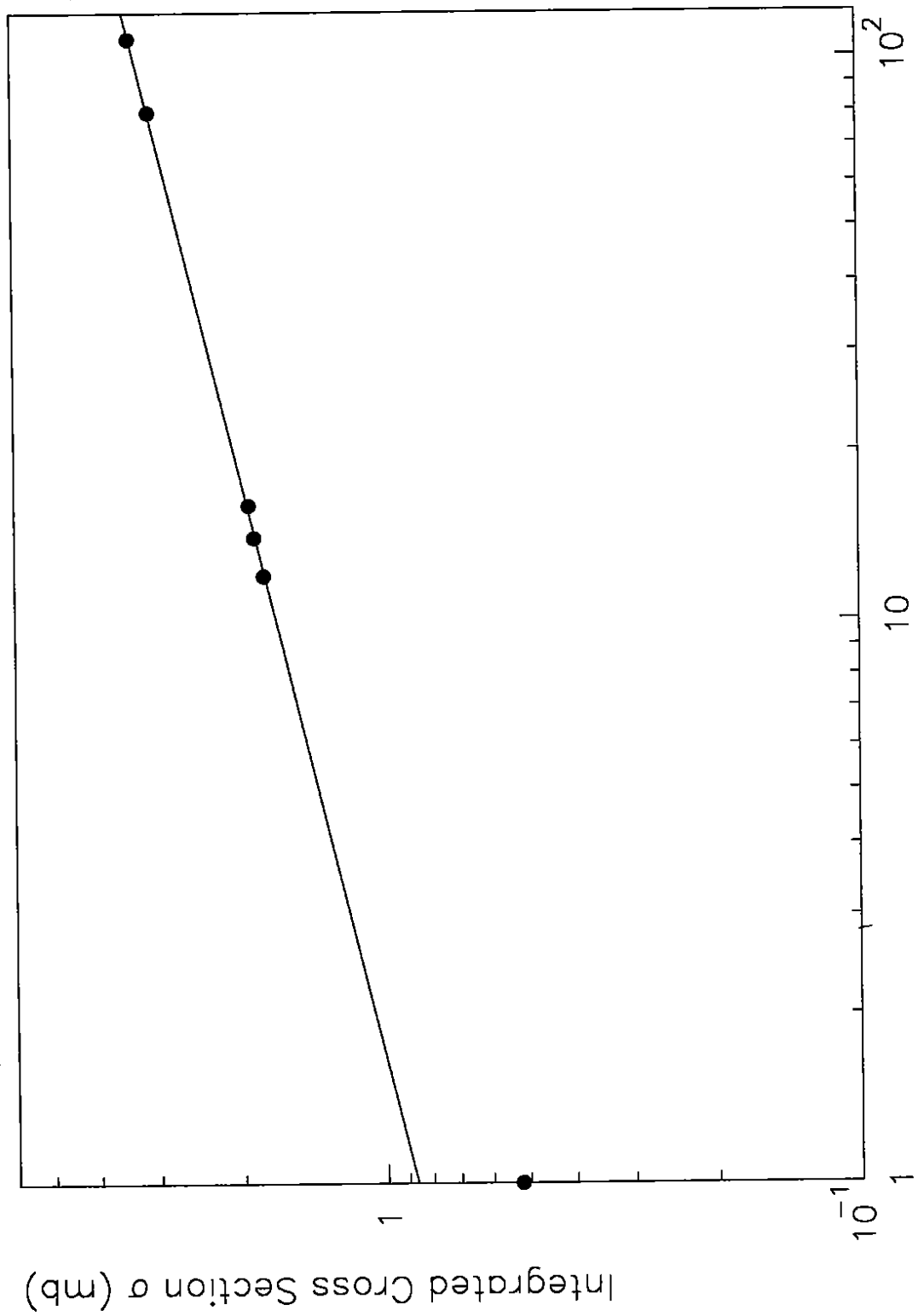


FIG. 3 Target Nucleon Number A